Published in final edited form as:
J Cell Physiol. 2012 March ; 227(3): 1062–1070. doi:10.1002/jcp.22819.

Aryl Hydrocarbon Receptor-Mediated Impairment of Chondrogenesis and Fracture Healing by Cigarette Smoke and Benzo(α)pyrene

Ming H. Kung[1,2], **Kiminori Yukata**[1], **Regis J. O'Keefe**[1], and **Michael J. Zuscik**[1]

[1]Department of Orthopaedics, Center for Musculoskeletal Research, University of Rochester Medical Center, 601 Elmwood Avenue, Box 665, Rochester, NY 14642

[2]Department of Environmental Medicine, Center for Musculoskeletal Research, University of Rochester Medical Center, 601 Elmwood Avenue, Box 665, Rochester, NY 14642

Abstract

The clinical literature strongly suggests that bone healing in cigarette smokers is impaired. Since cigarette smoke (CS) contains numerous polycyclic aromatic hydrocarbons (PAHs), and since dioxins impair bone formation *in vivo* via the Aryl Hydrocarbon Receptor (AHR), we investigated the impact of PAH/AHR signaling on chondrogenesis and on healing in a mouse tibial fracture model. We established that CS activates AHR signaling in fractures by up-regulating the AHR target gene *cytochrome p4501A1* (*Cyp1A1*). For in vitro studies, we employed the mouse limb bud micromass chondrogenesis model. After confirming that chondrocytes express AHR during differentiation, we treated cells with a prototypical PAH found in CS, benzo(α)pyrene (BaP), or cigarette smoke extract (CSE). Both BaP and CSE both strongly inhibited chondrogenesis in mesenchymal cells generated from E11 limb buds, with BaP also accelerating chondrocyte hypertrophy in cultures generated from E12 limb buds. Detection of DNA adducts in the BaP-treated cultures suggests that the distinct phenotypic effects of BaP may be due to the formation of reactive metabolites. Blockade of AHR signaling with the AHR antagonist MNF reverses the effects of BaP, but not CSE, suggesting that CSE inhibition of chondrogenesis is AHR-independent. Correlating with these results, tibial fracture calluses from BaP-treated mice were smaller and contained less mineralized tissue than vehicle controls. Overall, BaP is identified as a potent inhibitor of chondrogenesis *in vitro* with correlated effects on fracture healing similar to those of CS itself, suggesting a basis for PAHs as key compounds in the influence of CS on fracture repair.

Keywords

Aryl Hydrocarbon Receptor; Cigarette smoking; Chondrogenesis; Fracture healing

Introduction

While it is known that toxicants such as lead, cadmium, alcohol, and cigarette smoke (CS) can negatively impact bone health, their effects on chondrogenesis and endochondral ossification are poorly understood. In addition to the established role of smoking in pulmonary/cardiovascular disease and cancer, it is also a risk factor for skeletal disorders

Correspondence: Ming Kung, Departments of Orthopaedics & Environmental Medicine, Center for Musculoskeletal Research, University of Rochester Medical Center, 601 Elmwood Avenue, Box EHSC, Rochester, NY 14642, Office phone: 585-273-2197 Fax: 585-275-1121, ming_kung@urmc.rochester.edu.

including osteoporosis, disc disease, delayed fracture healing, and fracture nonunion (McKee et al., 2003; Porter and Hanley, 2001; Uei et al., 2006). The molecular mechanism(s) of these effects are unknown, but could be due to any of the more than 4,000 compounds present in CS (2010).

Endochondral ossification is the process of bone formation through a cartilage intermediate that occurs in growing long bones and during fracture healing (Einhorn, 1998; Gerstenfeld et al., 2003). Chondrogenesis is the first step, with mesenchymal progenitors proliferating and differentiating into chondrocytes. Chondrocyte hypertrophy and apoptosis follows. All steps are marked by the intricately controlled expression of stage-specific differentiation markers. In chondroprogenitors, the transcription factors Sox9 and hypoxia-inducible factor I (HIF1) control chondrogenesis and drive expression of matrix genes including type II collagen (Col2) and aggrecan. During terminal hypertrophy, chondrocytes express later markers including type X collagen (ColX) and alkaline phosphatase (ALP) (Goldring et al., 2006).

In vivo data suggest that CS affects chondrocyte differentiation, with intermittent smoke exposure inhibiting repair during distraction osteogenesis in rabbits (Ueng et al., 1997) and fracture healing in mice (El-Zawawy et al., 2006). The latter study demonstrated that smoke-exposed mice had a reduced amount of callus during early healing, potentially due to delayed chondrogenesis (El-Zawawy et al., 2006). CS contains several thousand compounds that could be responsible for this effect, including dozens of polycyclic aromatic hydrocarbons (PAHs) (Rubin, 2001). Many PAHs exert biological effects through activation of the aryl hydrocarbon receptor (AHR), a nuclear receptor that, upon activation, drives transcription of genes containing consensus AHR Response Elements (Kasai et al., 2006). A key target gene specifically trans-activated by AHR signaling is Cytochrome p4501A1 (Cyp1A1), one of several enzymes implicated in the bioactivation of benzo(α)pyrene (BaP), a PAH present in CS.

Dioxins exert deleterious effects on the skeleton during development (Hermsen et al., 2008), postnatally (Nishimura et al., 2009) and in mature vertebrates (Lind et al., 2009). Based on this, we suggest that dioxin-like compounds in CS induce AHR signaling which impacts the bone repair process at least partially via inhibition of chondrogenesis (El-Zawawy et al., 2006). We have employed the embryonic limb bud micromass chondrogenesis model (Zhang et al., 2004) and show that BaP inhibits mesenchymal cell chondrogenic commitment in an AHR-dependent manner while accelerating hypertrophy in committed chondrocytes. Furthermore, we present the results of a pilot tibial fracture study in mice administered BaP and conclude that changes in the callus architecture, including a reduced volume of mineralized callus, correlate with the published effects of CS on a similar mouse model of fracture healing (El-Zawawy et al., 2006). Our collective findings, which indicate that BaP can influence chondrocyte differentiation and reduce the amount of mineralized callus during fracture healing, implicate PAHs as key molecular players in the influence of CS on the skeletal repair process.

Materials and Methods

Animals

All mice used in this study were cared for according to the regulations the University of Rochester Medical Center Institutional Animal Care and Use Committee. Fractures were performed on 12 week old male C57/BL6 mice (Jackson Research Labs, Bar Harbor, ME). Timed pregnant dams (Jackson Research Labs) provided embryos at stage E11 or E12 for the generation of limb bud MSCs.

Fracture surgeries

Closed femoral fractures were created in the right hind limb in each mouse using an Einhorn Device (Bonnarens and Einhorn, 1984) as previously described (Naik et al., 2009). For tibial fractures, a 6 mm long incision was made in the skin on the anterior side of the tibia. A sterile 0.25 mm pin was inserted into the tibial marrow cavity, temporarily withdrawn to facilitate transection of the tibia with a scalpel at mid-shaft, and then reinserted. The incision was closed with 3 USP 5-0 sutures.

Smoke exposure

Mice administered mainstream CS on day 7 post-fracture received whole body exposure to smoke from research grade cigarettes (1R3F, University of Kentucky Tobacco-Health Research Program) generated using a Baumgartner-Jaeger CSM2072i cigarette smoking machine. The exposure was carried out by the Core Cigarette Smoke Exposure facility at the University of Rochester Medical Center using a protocol which closely mimics the pattern of smoking in humans consuming 20 cigarettes per day (Finch et al., 1998; Thatcher et al., 2005). Control mice were exposed to filtered room air in an identical chamber.

Tissue harvest from fractured mice

In mice administered femoral fractures, hind limbs were removed, dissected free from soft tissue and intramedullary pins were removed 2 hrs after smoke exposure. Fracture calluses were excised, flushed of marrow, and flash frozen in liquid nitrogen for mRNA extraction. Tissues were fixed in 10% neutral-buffered formalin (NBF) for 72 hrs followed by preservation in 70% EtOH prior to microCT analysis. A subset of tibiae were used to harvest fracture callus mRNA as described for femoral fractures.

Reagents

BaP (Sigma Aldrich, St. Louis, MO) and TCDD (Cambridge Isotopes, Cambridge, MA) were dissolved in DMSO to generate 10 mM stocks which were diluted to working concentrations in culture media for *in vitro* experiments. BaP was diluted in corn oil for intraperitoneal injection into mice undergoing fracture. 5 mM stocks of 3-methoxy-4-nitroflavone (MNF, provided by Dr. Thomas Gasiewicz, University of Rochester) were diluted to working concentrations in culture media. Aqueous CSE was prepared from 1R3F cigarettes using a modification of a previously published technique (Carp and Janoff, 1978).

Preparation of limb bud MSCs

Stage E11 and E12 mouse limb bud MSCs were prepared by enzymatic digestion of limb bud tissue as we have previously described (Zhang et al., 2004). Liberated MSCs were washed several times in serum-free DMEM and cultured in micromass (10^5 cells/10 μl) using a DME/F12 mixture (40%/60%, GIBCO, Grand Island, NY) supplemented with 10% FBS.

Cartilage nodule formation

After 5 or 7 days, micromass cultures were washed with PBS, fixed with 10% NBF (VWR, Buffalo Grove, IL) and rinsed with PBS. Each micromass was stained for 2 hrs at room temperature with a 3% alcian blue (Sigma, St. Louis, MO) solution. After washes, micromasses were photographed. Staining was quantified by dissolving the proteoglycan matrix with 4 M guanidine HCl (Sigma) and measuring OD_{595} using a plate reader.

RNA isolation

Frozen fracture calluses were homogenized using the Tissuelyser II system (Qiagen, Valencia, CA), and mRNA was isolated using the RNeasy Fibrous Tissue mini kit (Qiagen). Micromass mRNA was prepared using the PureLink™ Micro-to-Midi total RNA purification system (Invitrogen, Carlsbad, CA).

Quantitative PCR

mRNA was reverse transcribed into cDNA using the iScript cDNA synthesis kit (Bio-Rad, Hercules, CA) and qPCR was performed using the Rotor Gene Real-Time DNA Amplification System (Corbett Research, Sydney, Australia). cDNA samples were combined in a 20μL final volume with 1 mM primers (Table 1) and SYBR Green PCR Master Mix (Applied Biosystems, Foster City, CA). Dilutions of the cDNA pool were used for each primer set to generate a standard curve and data were normalized to *β-actin* expression for each sample.

SDS PAGE and Western blotting

Cells were lysed in freshly prepared RIPA lysis buffer containing 0.1% Halt protease inhibitor cocktail (Pierce, Rockford, IL). Protein concentration was determined using the BCA protein assay kit (Pierce). Protein extracts were fractionated by SDS-PAGE and electrophoretically transferred onto PVDF membranes. Membranes were blocked with 5% milk in TBST and then were incubated at 4°C overnight with antibodies against cytochrome p450A1 (Cyp1A1, Santa Cruz Biotechnology, Santa Cruz, CA), AHR (BioMol, Plymouth Meeting, PA), ARNT (Santa Cruz Biotechnology) or β-Actin (Sigma). After washing, membranes were incubated with secondary HRP-conjugated antibodies (Bio-Rad) for 1 hr at 20°C. Bands were visualized using the ECL kit (Pierce) using X-OMAT AR film (Kodak, Rochester, NY).

Cell viability and apoptosis

MSC viability was assessed using the Cell Titer Blue assay kit (Promega, Madison, WI), and apoptosis was assessed using the Vybrant apoptosis assay #4 (Invitrogen, Carlsbad, CA). For apoptosis assays, MSCs were resuspended via a 25 min incubation using 0.11 U dispase (Sigma) diluted in 500μl PBS containing 2% chick serum. Cells were counted, stained, and 3×10^6 cells/experimental condition were analyzed on a flow cytometer.

Histology/Immunohistochemistry

Micromasses were fixed in 10% NBF and paraffin-embedded. Sections (4 μm) were cut and stained with a monoclonal anti-mouse antibody specific for BPDE-DNA adduct (Santa Cruz) or matched isotype control antibody. The primary antibody was visualized with an HRP-conjugated rabbit anti-goat antibody (Jackson ImmunoResearch Laboratories). Sections were counterstained with hematoxylin. For tibiae, 3 mm sections were cut and stained with Alcian Blue/Hematoxylin/Orange G (ABH) according to standard protocols.

MicroCT assessment of mineralized fracture callus

Fracture calluses in BaP-exposed mice were evaluated via microCT using a Scanco vivaCT40 scanner with a 55 kVp source as we have previously described (Naik et al., 2009; Wu et al., 2008). Tibiae were scanned at a resolution of 12 μm with a slice increment of 10 μm. Images were reconstructed at identical thresholds to allow 3-dimensional structural rendering of the calluses.

Statistical analysis

Significant differences between experimental groups were identified using either a two-tailed Student's t-test or ANOVA. Differences between groups were considered significant when $p < 0.05$. Figures are presented as the mean +/− SEM.

Results

Aryl Hydrocarbon Receptor is activated in fracture callus of mice exposed to CS

In order to assess whether PAHs reach the fracture callus and thus could directly affect healing, we examined *Cyp1A1* expression 7 days following induction of femur fracture. Two hours after exposure of mice to mainstream CS, we isolated callus mRNA and performed RT-PCR to assess *Cyp1A1* expression. In 9/9 smoke-exposed mice, *Cyp1A1* mRNA was detectable, whereas in 8/8 air-treated mice, there was no detectable *Cyp1A1* product formed (Figure 1). These findings confirm that compounds in CS reach the fracture callus and activate AHR signaling. Given these findings, we set to determine the effect of PAH's on chondrogenesis, the first step in the fracture healing process.

Chondrocytes express a functional AHR

To determine whether chondrocytes support functional AHR signaling, AHR mRNA and protein expression was assessed in stage E11 limb bud MSCs. AHR mRNA and protein were expressed at low levels in undifferentiated cells on day 1, followed by a significant increase in expression during chondrogenesis, coinciding with up-regulation of key markers of chondrogenesis *Sox9* and *Col2* (Figure 2A and 2B). Comparatively, ARNT protein is constitutively expressed throughout chondrogenesis (Figure 2B). Together with the observed dose-dependent increases in Cyp1A1 protein induced by both TCDD and BaP (Figure 2C), this is the first report of functional AHR signaling in chondrocytes, representing a potential mechanism underlying the influence of PAHs on the initial step of fracture repair.

BaP inhibits chondrogenesis

We chose BaP it as a surrogate to investigate the effect of PAHs on chondrogenesis *in vitro*. We conducted initial experiments to determine if BaP affected the viability or apoptosis of MSCs. The highest doses of BaP (5 and 10 μM) did slightly reduce cell viability 24 hrs after treatment (Figure 3A), but had no impact on apoptosis 72 hrs after treatment (Figure 3B). Furthermore, continuous exposure of micromass cultures to 1 μM BaP did not significantly impact viability of the cells until the day 10 time point (Figure 3C). These results indicated that 1 μM BaP was safe for use in cultures of limb bud MSCs out to 7 days, establishing that effects of the toxicant during this time frame would not be due to reduced cell viability or increased apoptosis.

To assess the impact of BaP on chondrogenesis, stage E11 limb bud MSCs were employed because of their well established chondroprogenitor state (Clark et al., 2005; Zhang et al., 2004). Both 1 and 5 μM BaP significantly inhibited cartilage nodule formation at 7 days (Figure 4A), and the 1 μM dose also inhibited the expression of *Sox9* (Figure 4B) and *Col2* (Figure 4C). *Sox9* was inhibited at all time points out to 10 days and *Col2* expression was inhibited at days 5 and 10. These results indicate that BaP inhibits the process of chondrogenesis and suggests a possible influence of PAHs in general on the commitment of MSCs to the chondrocyte lineage.

BaP accelerates chondrocyte hypertrophy

To identify the impact of BaP on chondrocyte differentiation, we employed stage E12 murine limb bud cells, which are mostly comprised of committed chondrocytes in the

process of undergoing hypertrophic differentiation (Clark et al., 2005). While 1 μM BaP did not significantly impact *Col2* expression at any time point out to 10 days, *ColX* and *ALP* expression levels were both significantly increased (3–4 fold) at days 7 and 10 (Figure 5A–5C). These findings indicate that although BaP is an inhibitor of chondrogenesis, it accelerates hypertrophic differentiation in committed chondrocytes, further establishing complex and significant effects on processes involving chondrogenesis and chondrocyte differentiation.

Effects of BaP on chondrogenesis are AHR-dependent and involve DNA adduct formation

To confirm that BaP acts via the AHR, we blocked receptor signaling with the antagonist MNF (Lu et al., 1995). MNF dose-dependently reversed BaP inhibition of nodule formation in E11 limb bud MSCs (Figure 6A), thus implicating AHR signaling as the mechanism of action for BaP. Because AHR targets include various enzymes which can convert BaP into reactive metabolites, we also sought to determine whether BaP diol-epoxide-DNA adducts (BPDE) are formed in BaP-treated micromasses. Using an antibody that targets BPDE-DNA adducts, immunohistochemical assessment of micromasses revealed significant adduct formation in cultures exposed to 1 μM BaP for 7 days (Figure 6B). Overall, these findings indicate that BaP inhibits chondrogenesis in an AHR-dependent manner, and this may be due to the formation of reactive metabolites that lead to generalized genomic effects.

CSE inhibits chondrogenesis via an AHR-independent mechanism

CSE was employed to determine if the effects of smoke on chondrogenesis were similar to those of BaP. Interestingly, chronic treatment of stage E11 limb bud MSCs with varying doses of CSE for 5 days was found to significantly and dose-dependently inhibit chondrogenesis, evidenced by a significant reduction in nodule formation (Figure 7A). This effect was not due to generalized toxicity, evidenced 100% cell survival even after 7 days of exposure to CSE doses as high as 3% (Figure 7B). Interestingly, the AHR antagonist MNF did not reverse the inhibition of nodule formation by CSE, suggesting that the AHR does not mediate CSE action (Figure 7C). Furthermore, while both BaP and TCDD potently induced Cyp1A1, CSE did not induce this AHR target (Figure 7D). These findings suggest that at the doses investigated, the PAH fraction of CSE is not responsible for its inhibitory effects on chondrogenesis.

BaP alters callus architecture in mouse tibial fractures

It is established that CS reduces callus size in murine tibial fractures (El-Zawawy et al., 2006). To determine if PAHs underlie this effect, we assessed if BaP exposure induced a similar alteration in callus architecture. Mice administered tibial fractures were exposed daily to a physiologically relevant low dose (0.17 μg/kg/day) or high dose (1 mg/kg/day) BaP via IP injection. We detected a dose-dependent increase in *Cyp1A1*; whereas there was minimal detectable *Cyp1A1* product formed in vehicle-treated controls (Figure 8A) thus confirming BaP activation of AHR in the fracture callus. Radiographs from day 14 fractures (Figure 8B) and histology (Figure 8C) suggested reduced mineralized callus in BaP-exposed mice and were corroborated by microCT reconstructions (Figure 8D). microCT quantification established a significant reduction in mineralized callus volume in fractured mice administered BaP at all time points (Figure 8E). These results establish that BaP has a direct impact on fracture callus architecture, suggesting that PAHs in CS may be responsible for the altered healing in smokers.

Discussion

Smoking has been shown to have a negative impact on skeletal healing in a number of clinical situations. Smokers require 62% longer to heal tibial fractures (Schmitz et al., 1999)

and show delayed healing and a 4-fold increase in the rate of nonunion post-spinal fusion surgery (for review, (Porter and Hanley, 2001). Despite these significant clinical problems, there is no consensus as to the mechanism underlying the healing defect in smokers. The most widely studied molecule in this context is nicotine, which has been shown to inhibit distraction osteogenesis (Ma et al., 2007), spinal fusion (Silcox et al., 1995), and fracture healing in rabbits (Raikin et al., 1998). Conversely, CS, but not nicotine, has been shown to inhibit bone healing around a titanium implant in rabbits (Balatsouka et al., 2005a; Balatsouka et al., 2005b; Cesar-Neto et al., 2003). Furthermore, nicotine was not found to affect mechanical strength in a rat fracture model (Skott et al., 2006). Overall, these studies suggest that nicotine contributes to the effects of CS, but the conflicting results leave open the question about the exact nature of its contribution. The potential impact of other compounds in CS is unknown.

Of the myriad compounds in CS, dioxins are candidate effectors based on their ability to inhibit both osteoblast differentiation (Carpi et al., 2009; Korkalainen et al., 2009; Nishimura et al., 2009; Ryan et al., 2007) and osteoclast formation and differentiation (Korkalainen et al., 2009; Naruse et al., 2004; Voronov et al., 2005). Several risk factors have been implicated as inhibitors of bone repair specifically via impairment of chondrogenesis: corticosteroids (Gaston and Simpson, 2007), cyclooxygenase inhibition (Dimmen et al., 2009; Naik et al., 2009), and diabetes mellitus (Chaudhary et al., 2008). Furthermore, delayed chondrogenesis has been observed in smoke-exposed mice with tibial fractures (El-Zawawy et al., 2006). Thus, we have hypothesized that the PAH component of smoke may impair chondrogenesis via a mechanism mediated by the AHR.

There has been relatively little investigation into the non-carcinogenic toxicity of PAH's from smoke, particularly in tissues where cancer risk is not elevated. Following exposure of mice to mainstream CS (equivalent to 1 pack), AHR activation in the fracture callus by smoke was marked by induction of *Cyp1A1* (Figure 1). To our knowledge this is the first evidence that PAH's in smoke can reach the site of a fracture; in fact this is the first demonstration of AHR activation by CS at the site of *any* healing tissue apart from the lung. Sidestream smoke contains higher PAH levels than mainstream, suggesting risk to passive smokers as well (Lodovici et al., 2004). Regarding chondrocytes specifically, our findings are the first to identify a functional AHR signaling pathway which may mediate both toxic and physiological responses in chondrocytes. Not only does AHR mRNA and protein expression increase during chondrocyte differentiation, but there is also a signaling response to TCDD and BaP (Figure 2). It should be noted that differentiation-dependent regulation of AHR signaling has been established by our group in differentiating osteoblasts (Ryan et al., 2007), and in differentiating adipocytes (Shimba et al., 2003; Shimba et al., 2001). Overall, while the effects of smoke are likely to be multifactorial, our findings suggest AHR-mediated signaling is an underappreciated mechanism for some of the deleterious effects of PAHs in humans.

Findings presented here indicate that BaP inhibits chondrogenesis and accelerates chondrocyte differentiation in E11/E12 limb bud MSCs. This is in contrast to TCDD, which was found to be without effect on either of these processes (data not shown). BaP decreases cartilage nodule formation and decreases the expression of *Sox9* and *Col2* in stage E11 MSCs (Figure 4). Conversely, in committed chondrocytes derived from stage E12 limb buds, BaP up-regulates the expression of *ColX* and *ALP*, indicating acceleration of chondrocyte hypertrophy (Figure 5). Furthermore, the AHR antagonist MNF ameliorates the effects of BaP (Figure 6). Finally, we observed evidence of the formation of BPDE-DNA adducts (Figure 6), establishing that the influence of BaP is AHR-dependent and may be due to BaP bio-activation leading to DNA damage. Consistent with this, the delayed loss of cell viability seen following 10 days of BAP exposure (Figure 3C) is evidence for a slow

accumulation of DNA-damaging adducts that lead to cell death only after prolonged exposure. TCDD, unlike BaP, does not form reactive metabolites and does not affect chondrocyte differentiation (data not shown). These findings, which implicate DNA-damage caused by BaP metabolites as the basis for its effects on chondrocyte differentiation, suggest that this compound will impact fracture repair and thus represents an underlying contributor to the influence of CS on the healing process.

A mechanistic alternative to BaP induction of DNA damage is crosstalk between AHR signaling and other pathways that regulate chondrocyte differentiation. Several lines of evidence suggest a central role for HIF signaling during chondrogenesis with the consensus from these studies establishing HIF1 signaling as a requirement for chondrogenesis (Komatsu and Hadjiargyrou, 2004; Lafont et al., 2008; Provot et al., 2007; Schipani, 2005; Wang et al., 2007). HIF1 and AHR both require dimerization with ARNT for transcriptional activity, with several studies demonstrating inhibitory crosstalk between these two pathways (Allen et al., 2005; Chan et al., 1999; Khan et al., 2007). While further study is required, the impact of AHR signaling on chondrocyte differentiation may in part be a physiological consequence of crosstalk between these two pathways.

We employed a popular CSE model (Carp and Janoff, 1978) to study the *in vitro* effects of CS and have observed that this extract potently inhibits chondrogenesis in a manner similar to BaP (Figure 7A). However, inhibition of the AHR by MNF did not impact the influence of CSE on nodule formation (Figure 7C), and CSE did not induce Cyp1A1 (Figure 7D). Thus, the effects of CSE are not AHR-dependent and their molecular basis remains unidentified. Based on the finding that H_2O_2 inhibits chondrogenesis in chick limb bud micromass cultures (Zakany et al., 2005), it is possible that oxidants present in CSE are responsible for its effects. However, issues related to appropriate dosing and whether it accurately represents a surrogate for the smoke fraction reaching a distal tissue raises questions about its applicability as an *in vitro* reagent for studying CS exposure.

The *in vitro* findings presented in this manuscript support the emerging hypothesis that AHR signaling is a candidate molecular mechanism underlying the influence of CS on fracture repair. Since it is established that CS leads to the activation of the AHR in a healing fracture (Figure 1), an initial characterization of the impact of BaP on a murine tibial fracture model was performed. Results from this limited trial establish that both low and high doses of BaP effectively reduce the size of the mineralized callus at all time points of healing out to 21 days (Figure 8). This coincides with findings demonstrating that CS exposure of mice with tibial fractures leads to inhibited chondrogenesis and reduced overall callus size at 7 days (El-Zawawy et al., 2006). The general similarity between the two healing phenotypes suggest that BaP may indeed be a key molecular player in the influence of CS on fracture healing, setting the stage for more complete analysis of healing in BaP-treated mice, or in AHR-knockout mice (Lahvis and Bradfield, 1998; Walisser et al., 2005) that have been exposed to CS in a similar experimental fracture repair model.

To our knowledge, this study sets a new Lowest Observed Adverse Effect Level (LOAEL) for sub-chronic BaP exposure. The low dose studied (0.17 μg/kg/day) is near the estimated guideline dose of 0.08 μg/kg/day for cancer risk in humans (Fitzgerald et al., 2004). Our findings suggest that low doses of BaP and other PAHs may exert non-carcinogenic toxic effects by previously unappreciated mechanisms. Furthermore, these effects could manifest from exposures to a wide variety of environmental PAH sources. Together with evidence of AHR activation in the fracture callus by CS (Figure 1), this study raises the possibility that PAHs contribute to other pathologies associated with smoke. In conclusion, findings presented in this report establish that differentiating chondrocytes are susceptible to toxicity by AHR ligands. These effects may manifest during development and in adults during bone

repair. Inhibition of chondrogenesis by BaP is associated with induction of metabolizing enzymes, leading to bioactivation. With our evidence that CS can activate the AHR in the fracture callus, and that BaP can impact fracture callus architecture *in vivo*, a clear basis for further investigation of the BAP/smoke influence on skeletal repair is warranted.

Acknowledgments

The authors wish to thank Donna Hoak for excellent technical assistance in the preparation of limb bud MSC cultures and the University of Rochester Smoke Exposure Core, including Katherine Smolnycki and Dr. Thomas Thatcher. We also wish to acknowledge Dr. Thomas Gasiewicz for reagents and intellectual contributions to the study.

Contract grant sponsor: NIAMS

Contract grant number: R01 AR052011 (MJZ)

Contract grant sponsor: DOD

Contract grant number: W81XWH-06-1-0104 (MJZ)

Contract grant sponsor: NIEHS

Contract grant number: T32 AR053459

References

Allen JW, Johnson RS, Bhatia SN. Hypoxic inhibition of 3-methylcholanthrene-induced CYP1A1 expression is independent of HIF-1alpha. Toxicol Lett. 2005; 155(1):151–159. [PubMed: 15585370]

Balatsouka D, Gotfredsen K, Lindh CH, Berglundh T. The impact of nicotine on bone healing and osseointegration. Clin Oral Implants Res. 2005a; 16(3):268–276. [PubMed: 15877746]

Balatsouka D, Gotfredsen K, Lindh CH, Berglundh T. The impact of nicotine on osseointegration. An experimental study in the femur and tibia of rabbits. Clin Oral Implants Res. 2005b; 16(4):389–395. [PubMed: 16117761]

Bonnarens F, Einhorn TA. Production of a standard closed fracture in laboratory animal bone. J Orthop Res. 1984; 2(1):97–101. [PubMed: 6491805]

Carp H, Janoff A. Possible mechanisms of emphysema in smokers. In vitro suppression of serum elastase-inhibitory capacity by fresh cigarette smoke and its prevention by antioxidants. American Review of Respiratory Disease. 1978; 118:617–621. [PubMed: 101105]

Carpi D, Korkalainen M, Airoldi L, Fanelli R, Hakansson H, Muhonen V, Tuukkanen J, Viluksela M, Pastorelli R. Dioxin-sensitive proteins in differentiating osteoblasts: effects on bone formation in vitro. Toxicol Sci. 2009; 108(2):330–343. [PubMed: 19201780]

Cesar-Neto JB, Duarte PM, Sallum EA, Barbieri D, Moreno H Jr, Nociti FH Jr. A comparative study on the effect of nicotine administration and cigarette smoke inhalation on bone healing around titanium implants. JPeriodontol. 2003; 74(10):1454–1459. [PubMed: 14653391]

Chan WK, Yao G, Gu YZ, Bradfield CA. Cross-talk between the aryl hydrocarbon receptor and hypoxia inducible factor signaling pathways. Demonstration of competition and compensation. J Biol Chem. 1999; 274(17):12115–12123. [PubMed: 10207038]

Chaudhary SB, Liporace FA, Gandhi A, Donley BG, Pinzur MS, Lin SS. Complications of ankle fracture in patients with diabetes. J Am Acad Orthop Surg. 2008; 16(3):159–170. [PubMed: 18316714]

Clark CA, Schwarz EM, Zhang X, Ziran NM, Drissi H, O'Keefe RJ, Zuscik MJ. Differential regulation of EP receptor isoforms during chondrogenesis and chondrocyte maturation. Biochemical and Biophysical Research Communications. 2005; 328(3):764–776. [PubMed: 15694412]

Dimmen S, Nordsletten L, Madsen JE. Parecoxib and indomethacin delay early fracture healing: a study in rats. Clin Orthop Relat Res. 2009; 467(8):1992–1999. [PubMed: 19319614]

Einhorn TA. The cell and molecular biology of fracture healing. ClinOrthop. 1998; 355(Suppl):S7–21.

El-Zawawy HB, Gill CS, Wright RW, Sandell LJ. Smoking delays chondrogenesis in a mouse model of closed tibial fracture healing. Journal of Orthopaedic Research. 2006; 24(12):2150–2158. [PubMed: 17013832]

Finch GL, Lundgren DL, Barr EB, Chen BT, Griffith WC, Hobbs CH, Hoover MD, Nikula KJ, Mauderly JL. Chronic cigarette smoke exposure increases the pulmonary retention and radiation dose of 239Pu inhaled as 239PuO2 by F344 rats. Health Phys. 1998; 75(6):597–609. [PubMed: 9827506]

Fitzgerald DJ, Robinson NI, Pester BA. Application of benzo(a)pyrene and coal tar tumor dose-response data to a modified benchmark dose method of guideline development. Environ Health Perspect. 2004; 112(14):1341–1346. [PubMed: 15471723]

Gaston MS, Simpson AH. Inhibition of fracture healing. J Bone Joint Surg Br. 2007; 89(12):1553–1560. [PubMed: 18057352]

Gerstenfeld LC, Cullinane DM, Barnes GL, Graves DT, Einhorn TA. Fracture healing as a post-natal developmental process: molecular, spatial, and temporal aspects of its regulation. JCell Biochem. 2003; 88(5):873–884. [PubMed: 12616527]

Goldring MB, Tsuchimochi K, Ijiri K. The control of chondrogenesis. JCell Biochem. 2006; 97(1):33–44. [PubMed: 16215986]

Hermsen SA, Larsson S, Arima A, Muneoka A, Ihara T, Sumida H, Fukusato T, Kubota S, Yasuda M, Lind PM. In utero and lactational exposure to 2,3,7,8-tetrachlorodibenzo-p-dioxin (TCDD) affects bone tissue in rhesus monkeys. Toxicology. 2008; 253(1–3):147–152. [PubMed: 18835322]

IARC. Some non-heterocyclic polycyclic aromatic hydrocarbons and some related exposures. IARC Monogr Eval Carcinog Risks Hum. 2010; 92:1–853. [PubMed: 21141735]

Kasai A, Hiramatsu N, Hayakawa K, Yao J, Maeda S, Kitamura M. High levels of dioxin-like potential in cigarette smoke evidenced by in vitro and in vivo biosensing. Cancer Res. 2006; 66(14):7143–7150. [PubMed: 16849560]

Khan S, Liu S, Stoner M, Safe S. Cobaltous chloride and hypoxia inhibit aryl hydrocarbon receptor-mediated responses in breast cancer cells. Toxicol Appl Pharmacol. 2007; 223(1):28–38. [PubMed: 17599377]

Komatsu DE, Hadjiargyrou M. Activation of the transcription factor HIF-1 and its target genes, VEGF, HO-1, iNOS, during fracture repair. Bone. 2004; 34(4):680–688. [PubMed: 15050899]

Korkalainen M, Kallio E, Olkku A, Nelo K, Ilvesaro J, Tuukkanen J, Mahonen A, Viluksela M. Dioxins interfere with differentiation of osteoblasts and osteoclasts. Bone. 2009; 44(6):1134–1142. [PubMed: 19264158]

Lafont JE, Talma S, Hopfgarten C, Murphy CL. Hypoxia promotes the differentiated human articular chondrocyte phenotype through SOX9-dependent and -independent pathways. J Biol Chem. 2008; 283(8):4778–4786. [PubMed: 18077449]

Lahvis GP, Bradfield CA. Ahr null alleles: distinctive or different? Biochemical Pharmacology. 1998; 56(7):781–787. [PubMed: 9774139]

Lind PM, Wejheden C, Lundberg R, Alvarez-Lloret P, Hermsen SA, Rodriguez-Navarro AB, Larsson S, Rannug A. Short-term exposure to dioxin impairs bone tissue in male rats. Chemosphere. 2009; 75(5):680–684. [PubMed: 19152955]

Lodovici M, Akpan V, Evangelisti C, Dolara P. Sidestream tobacco smoke as the main predictor of exposure to polycyclic aromatic hydrocarbons. J Appl Toxicol. 2004; 24(4):277–281. [PubMed: 15300715]

Lu YF, Santostefano M, Cunningham BD, Threadgill MD, Safe S. Identification of 3′-methoxy-4′-nitroflavone as a pure aryl hydrocarbon (Ah) receptor antagonist and evidence for more than one form of the nuclear Ah receptor in MCF-7 human breast cancer cells. Arch Biochem Biophys. 1995; 316(1):470–477. [PubMed: 7840652]

Ma L, Zheng LW, Cheung LK. Inhibitory effect of nicotine on bone regeneration in mandibular distraction osteogenesis. Front Biosci. 2007; 12:3256–3262. [PubMed: 17485296]

McKee MD, DiPasquale DJ, Wild LM, Stephen DJ, Kreder HJ, Schemitsch EH. The effect of smoking on clinical outcome and complication rates following Ilizarov reconstruction. J Orthop Trauma. 2003; 17(10):663–667. [PubMed: 14600564]

Naik AA, Xie C, Zuscik MJ, Kingsley P, Schwarz EM, Awad H, Guldberg R, Drissi H, Puzas JE, Boyce B, Zhang X, O'Keefe RJ. Reduced COX-2 expression in aged mice is associated with impaired fracture healing 18. Journal of Bone and Mineral Research. 2009; 24(2):251–264. [PubMed: 18847332]

Naruse M, Otsuka E, Ishihara Y, Miyagawa-Tomita S, Hagiwara H. Inhibition of osteoclast formation by 3-methylcholanthrene, a ligand for arylhydrocarbon receptor: suppression of osteoclast differentiation factor in osteogenic cells. Biochem Pharmacol. 2004; 67(1):119–127. [PubMed: 14667934]

Nishimura N, Nishimura H, Ito T, Miyata C, Izumi K, Fujimaki H, Matsumura F. Dioxin-induced up-regulation of the active form of vitamin D is the main cause for its inhibitory action on osteoblast activities, leading to developmental bone toxicity. Toxicol Appl Pharmacol. 2009; 236(3):301–309. [PubMed: 19367694]

Porter SE, Hanley EN Jr. The musculoskeletal effects of smoking. J Am Acad Orthop Surg. 2001; 9(1):9–17. [PubMed: 11174159]

Provot S, Zinyk D, Gunes Y, Kathri R, Le Q, Kronenberg HM, Johnson RS, Longaker MT, Giaccia AJ, Schipani E. Hif-1alpha regulates differentiation of limb bud mesenchyme and joint development. J Cell Biol. 2007; 177(3):451–464. [PubMed: 17470636]

Raikin SM, Landsman JC, Alexander VA, Froimson MI, Plaxton NA. Effect of nicotine on the rate and strength of long bone fracture healing. ClinOrthop. 1998; (353):231–237.

Rubin H. Synergistic mechanisms in carcinogenesis by polycyclic aromatic hydrocarbons and by tobacco smoke: a bio-historical perspective with updates. Carcinogenesis. 2001; 22(12):1903–1930. [PubMed: 11751421]

Ryan EP, Holz JD, Mulcahey M, Sheu TJ, Gasiewicz TA, Puzas JE. Environmental toxicants may modulate osteoblast differentiation by a mechanism involving the aryl hydrocarbon receptor. Journal of Bone and Mineral Research. 2007; 22(10):1571–1580. [PubMed: 17576166]

Schipani E. Hypoxia and HIF-1 alpha in chondrogenesis. Semin Cell Dev Biol. 2005; 16(4–5):539–546. [PubMed: 16144691]

Schmitz MA, Finnegan M, Natarajan R, Champine J. Effect of smoking on tibial shaft fracture healing. ClinOrthop. 1999; (365):184–200.

Shimba S, Hayashi M, Ohno T, Tezuka M. Transcriptional regulation of the AhR gene during adipose differentiation. Biol Pharm Bull. 2003; 26(9):1266–1271. [PubMed: 12951469]

Shimba S, Wada T, Tezuka M. Arylhydrocarbon receptor (AhR) is involved in negative regulation of adipose differentiation in 3T3-L1 cells: AhR inhibits adipose differentiation independently of dioxin. J Cell Sci. 2001; 114(Pt 15):2809–2817. [PubMed: 11683414]

Silcox DH III, Daftari T, Boden SD, Schimandle JH, Hutton WC, Whitesides TE Jr. The effect of nicotine on spinal fusion. Spine. 1995; 20(14):1549–1553. [PubMed: 7570168]

Skott M, Andreassen TT, Ulrich-Vinther M, Chen X, Keyler DE, LeSage MG, Pentel PR, Bechtold JE, Soballe K. Tobacco extract but not nicotine impairs the mechanical strength of fracture healing in rats. J Orthop Res. 2006; 24(7):1472–1479. [PubMed: 16705735]

Thatcher TH, McHugh NA, Egan RW, Chapman RW, Hey JA, Turner CK, Redonnet MR, Seweryniak KE, Sime PJ, Phipps RP. Role of CXCR2 in cigarette smoke-induced lung inflammation. AmJPhysiol Lung Cell MolPhysiol. 2005; 289(2):L322–L328.

Uei H, Matsuzaki H, Oda H, Nakajima S, Tokuhashi Y, Esumi M. Gene expression changes in an early stage of intervertebral disc degeneration induced by passive cigarette smoking. Spine (Phila Pa 1976). 2006; 31(5):510–514. [PubMed: 16508543]

Ueng SW, Lee MY, Li AF, Lin SS, Tai CL, Shih CH. Effect of intermittent cigarette smoke inhalation on tibial lengthening: experimental study on rabbits. J Trauma. 1997; 42(2):231–238. [PubMed: 9042873]

Voronov I, Heersche JN, Casper RF, Tenenbaum HC, Manolson MF. Inhibition of osteoclast differentiation by polycyclic aryl hydrocarbons is dependent on cell density and RANKL concentration. Biochem Pharmacol. 2005; 70(2):300–307. [PubMed: 15919055]

Walisser JA, Glover E, Pande K, Liss AL, Bradfield CA. Aryl hydrocarbon receptor-dependent liver development and hepatotoxicity are mediated by different cell types. Proc Natl Acad Sci U S A. 2005; 102(49):17858–17863. [PubMed: 16301529]

Wang Y, Wan C, Deng L, Liu X, Cao X, Gilbert SR, Bouxsein ML, Faugere MC, Guldberg RE, Gerstenfeld LC, Haase VH, Johnson RS, Schipani E, Clemens TL. The hypoxia-inducible factor alpha pathway couples angiogenesis to osteogenesis during skeletal development. J Clin Invest. 2007; 117(6):1616–1626. [PubMed: 17549257]

Wu Q, Kim KO, Sampson ER, Chen D, Awad H, O'Brien T, Puzas JE, Drissi H, Schwarz EM, O'Keefe RJ, Zuscik MJ, Rosier RN. Induction of an osteoarthritis-like phenotype and degradation of phosphorylated Smad3 by Smurf2 in transgenic mice. Arthritis and Rheumatism. 2008; 58(10): 3132–3144. [PubMed: 18821706]

Zakany R, Szijgyarto Z, Matta C, Juhasz T, Csortos C, Szucs K, Czifra G, Biro T, Modis L, Gergely P. Hydrogen peroxide inhibits formation of cartilage in chicken micromass cultures and decreases the activity of calcineurin: implication of ERK1/2 and Sox9 pathways. Exp Cell Res. 2005; 305(1): 190–199. [PubMed: 15777799]

Zhang X, Ziran N, Goater JJ, Schwarz EM, Puzas JE, Rosier RN, Zuscik M, Drissi H, O'Keefe RJ. Primary murine limb bud mesenchymal cells in long-term culture complete chondrocyte differentiation: TGF-beta delays hypertrophy and PGE2 inhibits terminal differentiation. Bone. 2004; 34(5):809–817. [PubMed: 15121012]

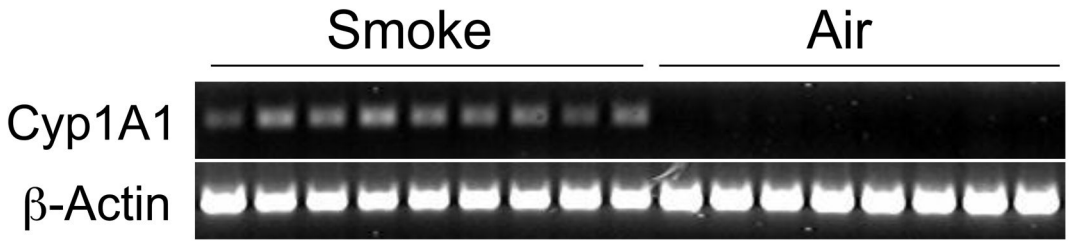

Figure 1. Cyp1A1 mRNA is induced in fracture callus of mice exposed to CS

Seventeen mice were administered tibial fractures. After 7 days of healing, fractured mice were exposed to either CS or room air. Two hours after exposure, mice were sacrificed and the fracture callus tissues were harvested. mRNA was extracted from each callus PCR was performed to assess *Cyp1A1* and *β-actin* expression. Products were run on an agarose gel and bands were visualized via ethidium bromide stain.

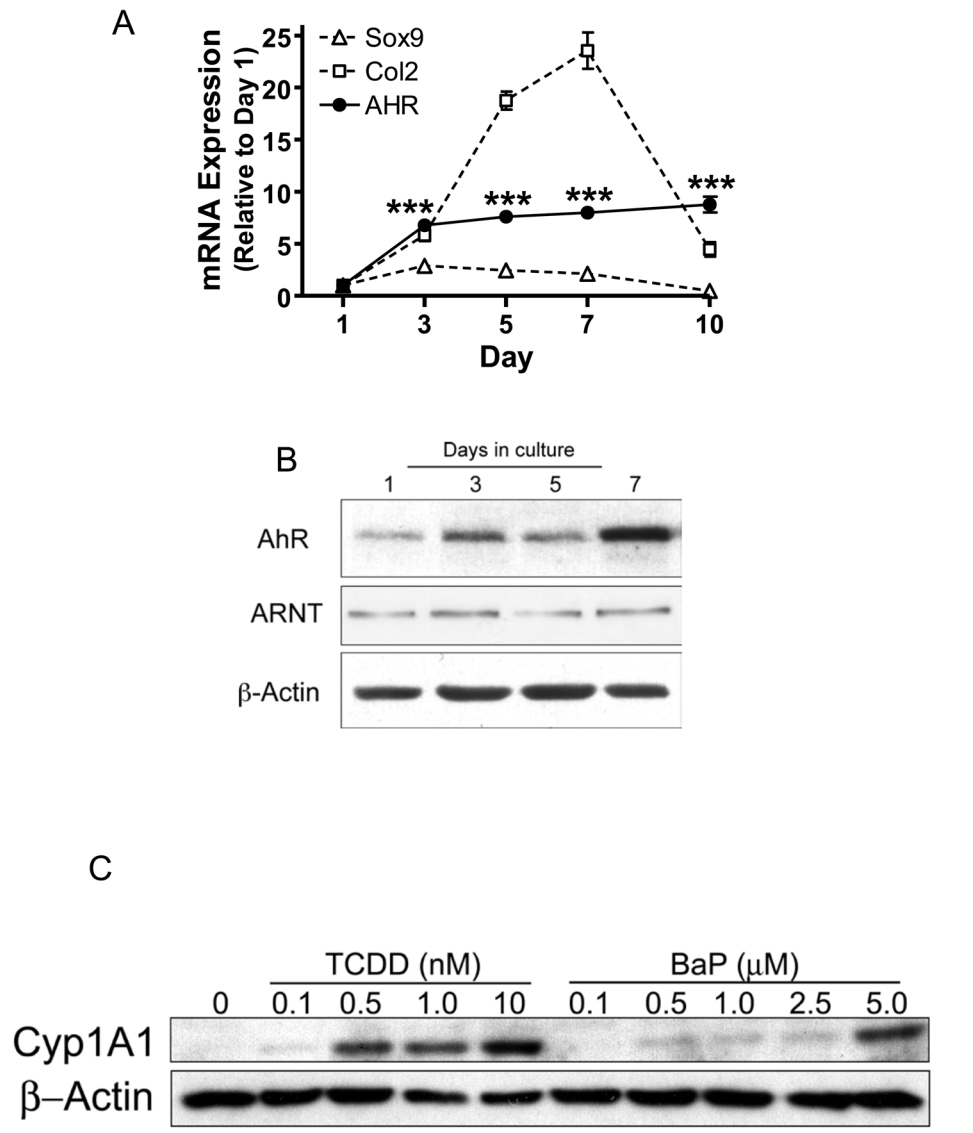

Figure 2. Functional AHR expression positively correlates with chondrocyte maturation

Stage E11 limb bud cells were seeded into micromass cultures. mRNA and protein were harvested at indicated time points. (**A**) qPCR was performed to detect *Sox9*, *Col2* and *AHR*. Expression was corrected for *βactin* expression and data were normalized to the day 1 time point. (N≥3, ***p<0.001, ANOVA). (**B**) Western blotting was performed to assess AHR and ARNT proteins levels during chondrogenesis usingβ-actin as a loading control. (**C**) After 7 days in culture, stage E11 limb bud micromass cultures were treated with varying doses of TCDD or BaP and proteins were harvested 12 hrs later. Expression of Cyp1A1 and β-actin were assessed by western blot. Blots shown are representative of findings from 3 separate experiments.

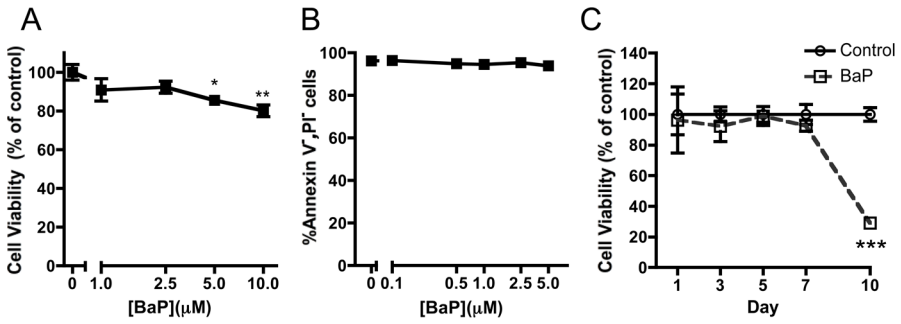

Figure 3. Relevant doses of BaP do not impact stage E11 limb bud MSC viability or apoptotic potential

(**A**) Stage E11 limb bud MSCs were cultured in micromass with varying doses of BaP. Following a 5 day exposure period, Cell Titer Blue cell viability assay was performed. (**B**). We assessed apoptosis using the Vybrant Apoptosis assay after 3 days in culture. (**C**) 1 μM BaP was added and we determined cell viability at indicated time points using Cell Titer Blue. (N=3, *p<0.05, **p<0.01, ***p<0.001, Student's t-test).

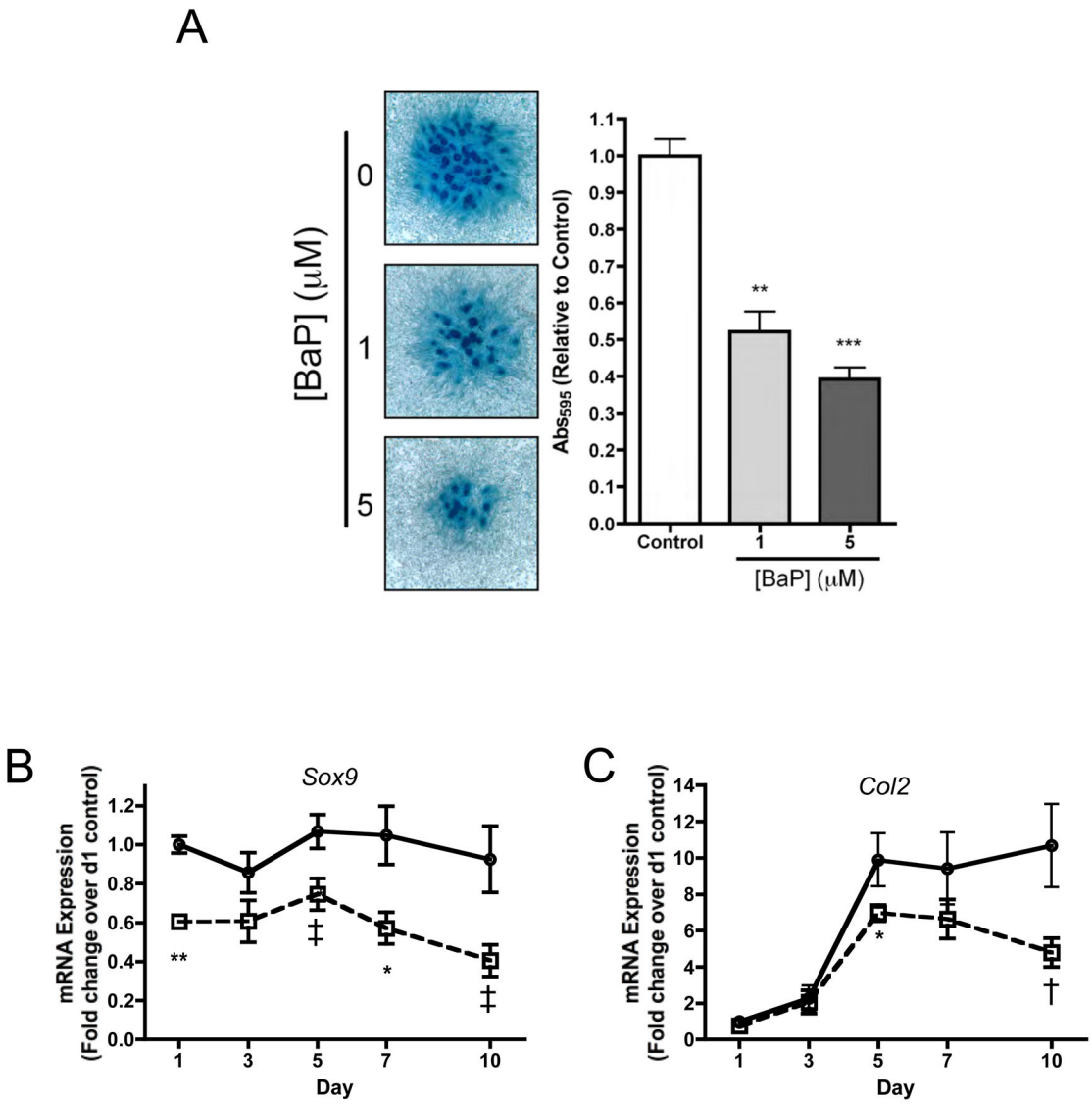

Figure 4. BaP inhibits chondrogenesis and chondrocyte differentiation in Stage E11 limb bud MSCs

(**A**) Stage E11 limb bud MSCs were cultured in micromass. Cultures were treated with BaP (or DMSO vehicle). On day 7, micromasses were stained with Alcian Blue. Staining intensity was quantified by dissolution of proteoglycan matrix followed by determination of OD_{595}. Bar=1mm. (**B** & **C**) Micromass cultures of stage E11 limb bud MSCs were treated with BaP and mRNA was harvested at indicated time points and qPCR was performed to quantify the expression of *Sox9* and *col2*. qPCR results were corrected for *β-actin* expression and normalized to the day 1 level for each gene (N=3, $^{\dagger}p$=0.72, $^{\ddagger}p$<0.055, *p<0.05, **p<0.01, Student's t-test).

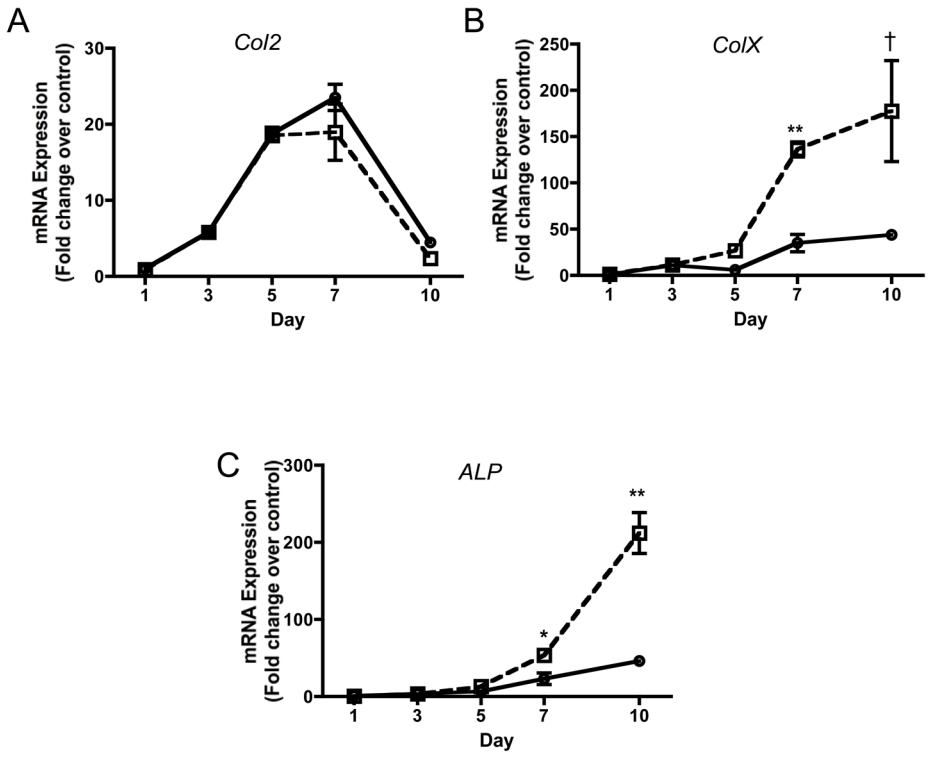

Figure 5. BaP stimulates chondrocyte maturation in Stage E12 limb bud chondrocytic cells

More mature limb bud cells harvested at stage E12 were cultured in micromass. Cultures were treated with 1μM BaP and mRNA was harvested at indicated time points. qPCR was performed to quantify the expression of *col2* (**A**), *colX* (**B**) and *ALP* (**C**). qPCR results were corrected for *β-actin* expression and normalized to the day 1 level for each gene (N=3, $^{\dagger}p$=0.071, *p<0.05, **p<0.01, Student's t-test).

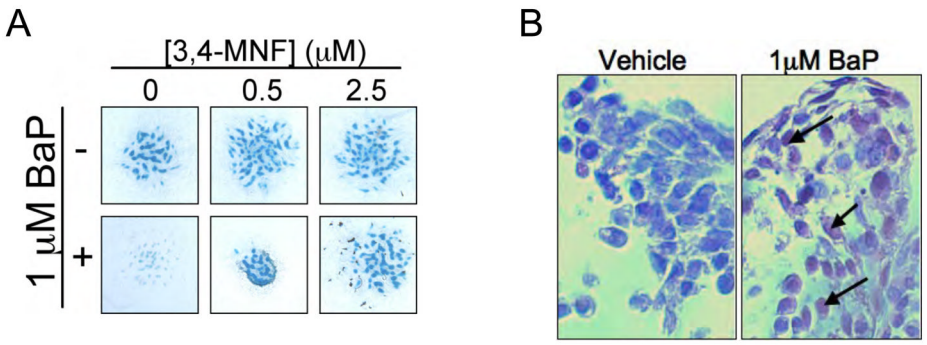

Figure 6. Effects of BaP on chondrogenesis are AHR dependent, and involve BPDE-DNA adduct formation

(**A**) Stage E11 limb bud MSCs were cultured in micromass and treated with 1 μM BaP (or vehicle) in the presence of varying doses (0, 0.5, 2.5 μM) of the AHR antagonist, 3,4-MNF and alcian blue staining was performed after 7 days. The experiment was repeated 3 times, with a representative panel of alcian blue-stained cultures shown. Bar=1mm. (**B**) Stage E11 limb bud MSCs were cultured in micromass for 7 days and then treated for 3 days with 1 μM BaP (or vehicle). Micromasses were then fixed, embedded in paraffin and immunohistochemistry was performed using a BPDE-DNA adduct-specific antibody. The experiment was repeated 3 times, with representative histology presented (Bar=25μM).

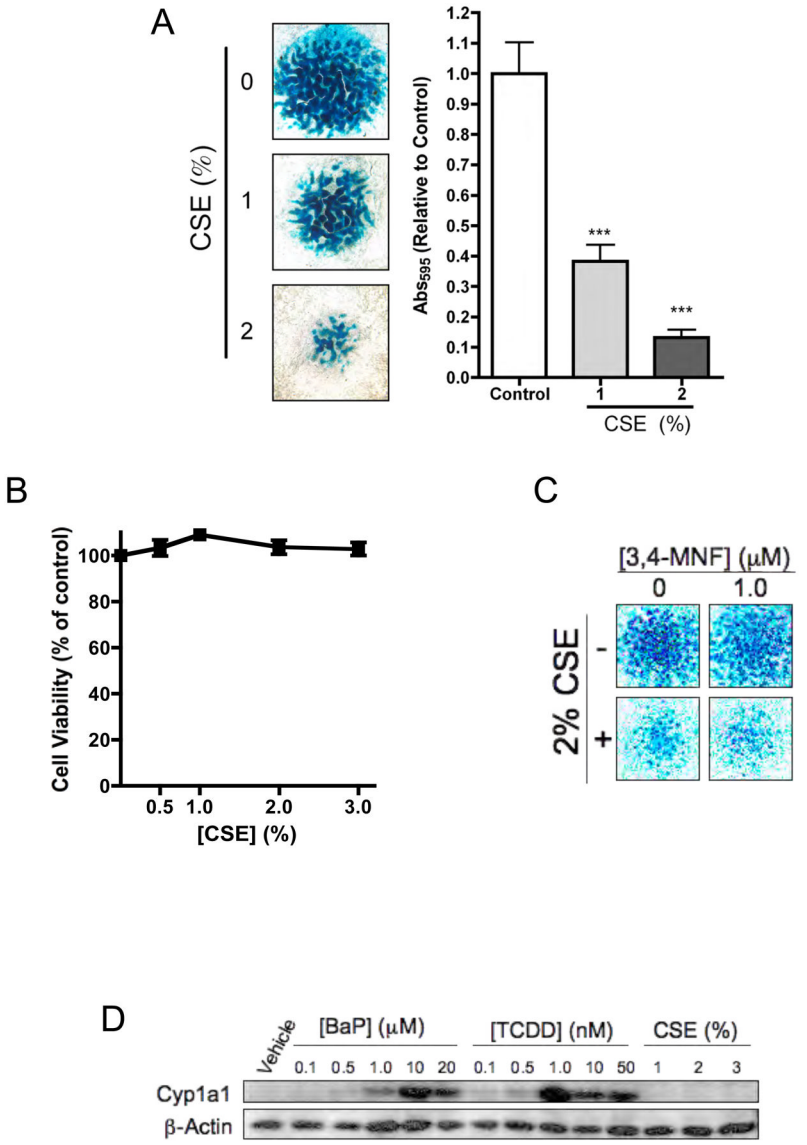

Figure 7. Inhibition of chondrogenesis by CSE is independent of AHR signaling

(**A**) To assess the effects of CSE on chondrogenesis, cultures were treated with 0, 1 or 2% CSE for 7 days and nodule formation was assessed via alcian blue staining. Staining intensity was quantified by dissolution of proteoglycan matrix followed by determination of OD_{595} (N=3, $^{**}P<0.01$, $^{***}P<0.001$). Bar=1mm. (**B**) To assess the impact of CSE on cell viability, stage E11 limb bud MSCs were cultured in micromass and were treated for 7 days with increasing concentrations of CSE. Cell viability was assessed via Cell Titer Blue assay (N≥3). (**C**) Micromass cultures were treated with 2% CSE (or vehicle) in the presence (1 μM) or absence of the AHR antagonist, 3,4-MNF and alcian blue staining was performed after 7 days. (**D**) After 7 days in culture, stage E11 limb bud micromass cultures were treated with varying doses of BaP, TCDD or CSE and proteins were harvested 12 hrs later. Western blotting was performed to assess the expression of Cyp1A1 and β-actin. In all cases, the data presented are representative of findings from at least 3 separate experiments. Bar=1mm.

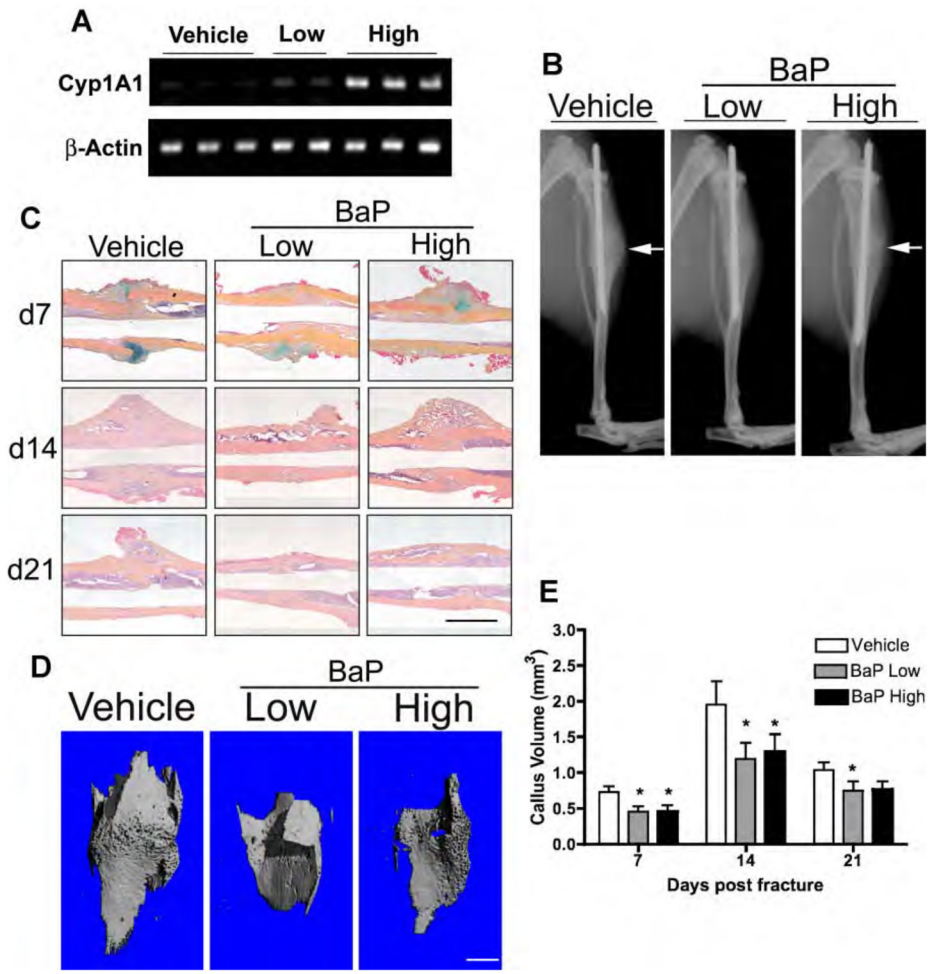

Figure 8. BaP reduces mineralized callus volume and accelerates cartilage hypertrophy in mouse tibial fractures

Ten week old male mice were given daily IP injection of low (0.17 μg/kg/day) or high (1 mg/kg/day) dose BaP or vehicle (corn oil) for 14 days prior to surgery. After tibial fracture surgery, treatment was continued up to 21 days. (**A**) mRNA was extracted from calluses 7 days post-fracture, 4 hrs after administration of BaP (or vehicle), and PCR was performed to assess *Cyp1A1* and*β-actin* expression. (**B**) Radiographs were collected from treated and control mice 14 days post-fracture. White arrows depict the location of the fracture and thus the location of the callus that has formed. (C) Tibial fractures were stained with ABH at the indicated time points, representative sections are displayed. Bar=1mm. (**D** & **E**) microCT analysis of mineralized callus volume was performed. Representative reconstructions of mineralized callus at 14 days post-fracture are depicted in (**D**) and quantification of mineralized callus volume at 7, 14 and 21 days post-fracture is presented in (**E**). (N≥3, **P*<0.05, Student's t-test). Bar=1mm.

TABLE 1

Primers sets used for RT-PCR

Gene	Forward Primer	Reverse Primer
Sox9	AGGAAGCTGGCAGACCAGTA	GTCCGTTCTTCACCGACTTC
Col2a1	AGAACAGCATCGCCTACCTG	CTTGCCCCACTTACCAGTGT
ColX	CATAAAGGGCCCACTTGCTA	CCTGGCTCTCCTTGGAGTC
Actin	AGAGGGAAATCGTGCGTGAC	ATGCCACAGGATTCCATACC
AHR	CATGGAGAGGTGCTTCAGGT	TTCGAATTTCCAGGATGGAG
Cyp1A1	CCTCTTTGGAGCTGGGTTTG	CGGAAGGTCTCCAGAATGAA
Alkaline Phosphatase	TGACCTTCTCTCCTCCATCC	CTTCCTGGGAGTCTCATCCT
Osteocalcin	AGGGAGGATCAAGTCCCG	GAACAGACTCCGGCGCTA